Journal of Colloid and Interface Science 483 (2016) 334–342

Contents lists available at ScienceDirect

Journal of Colloid and Interface Science

journal homepage: www.elsevier.com/locate/jcis

Regular Article

The specific sorption of Np(V) on the corundum (α-Al_2O_3) surface in the presence of trivalent lanthanides Eu(III) and Gd(III): A batch sorption and XAS study

S. Virtanen [a,*], F. Bok [b], A. Ikeda-Ohno [b], A. Rossberg [b], J. Lützenkirchen [c], T. Rabung [c], J. Lehto [a], N. Huittinen [b]

[a] Laboratory of Radiochemistry, Department of Chemistry, University of Helsinki, P.O. Box 55, 00014 University of Helsinki, Finland
[b] Helmholtz-Zentrum Dresden-Rossendorf, Institute of Resource Ecology, Bautzner Landstrasse 400, 01328 Dresden, Germany
[c] Institut für Nukleare Entsorgung, Karlsruhe Institute of Technology, P.O. Box 3640, 76021 Karlsruhe, Germany

GRAPHICAL ABSTRACT

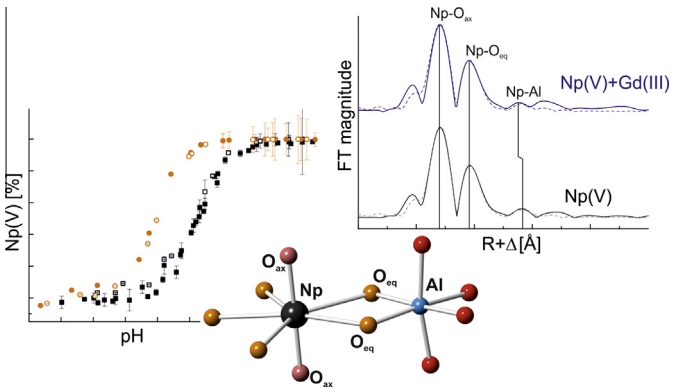

ARTICLE INFO

Article history:
Received 29 April 2016
Revised 4 August 2016
Accepted 12 August 2016
Available online 13 August 2016

Keywords:
Np(V)
Eu(III)
Gd(III)
Sorption competition
Batch sorption
X-ray absorption spectroscopy

ABSTRACT

The sorption of pentavalent neptunium, Np(V), on corundum (α-Al_2O_3) was investigated in the absence and presence of trivalent europium or gadolinium as a competing element under CO_2-free conditions. The objective of this study was to investigate how a trivalent metal ion with a higher charge than that of the neptunyl(V) ion would affect the sorption of Np(V) when allowed to adsorb on the mineral surface before the addition of Np(V). Batch sorption experiments conducted as a function of pH (pH-edges) and as a function of Np(V) concentration (isotherms) in the absence and presence of 1×10^{-5} M Eu(III) showed no sign of Eu being able to block Np sorption sites. Surface complexation modelling using the diffuse double layer model was applied to the batch data to obtain surface complexation constants for the formed Np(V) complexes on corundum. To account for potential changes occurring in the coordination environment of the neptunium ion in the presence of a trivalent lanthanide, X-ray absorption spectroscopy (XAS) measurements were carried out on the samples containing only Np(V) and Np(V) + Gd(III). The results reveal the presence of a bidentate Np(V) edge-sharing complex on the corundum surface in the absence of Gd(III), while the coordination environment of Np(V) on the corundum surface could be changed when Gd(III) is added to the sample before the sorption of Np(V).

* Corresponding author.
E-mail addresses: sinikka.m.virtanen@helsinki.fi (S. Virtanen), f.bok@hzdr.de (F. Bok), a.ikeda@hzdr.de (A. Ikeda-Ohno), rossberg@esrf.fr (A. Rossberg), johannes.luetzenkirchen@kit.edu (J. Lützenkirchen), thomas.rabung@kit.edu (T. Rabung), jukka.lehto@helsinki.fi (J. Lehto), n.huittinen@hzdr.de (N. Huittinen).

http://dx.doi.org/10.1016/j.jcis.2016.08.035
0021-9797/

1. Introduction

In many countries the final disposal of spent nuclear fuel (SNF) in different geological host rock formations, such as clay, salt, and crystalline rock, will take place during the next few decades, starting in Finland from 2020. To account for the safety of these SNF repositories various radionuclide (RN) release scenarios and the subsequent transport of RNs by ground water or their retention on solid surfaces have to be considered. RN uptake studies, where sorption distribution coefficients (K_d or R_d values) onto essential metal retaining surfaces present in the near- and far fields of the candidate host rock formations are determined, are often conducted using a single element at a time. In reality, however, there is a wide variety of other dissolved radioactive and stable elements in different concentrations present that could compete for mineral surface sites and, thus, affect the extent of retardation of the radionuclides released from the SNF over time. The understanding of competitive sorption reactions and their causes is vital when drawing conclusions about complex environmental systems, such as the sorption of radionuclides in bedrock [1,2], which is of importance when assessing nuclear waste disposal safety. Despite this, only a limited amount of literature is available on RN sorption competition reactions on solid surfaces.

In competitive sorption investigations by Bradbury and Baeyens [3], metal ion competition for sorption sites on montmorillonite was found to occur when two metals with the same oxidation state and similar hydrolysis behavior were present simultaneously in the montmorillonite suspension. The authors found that trivalent metals Eu(III), Nd(III) and Am(III) show clear competitive effects when added together, as do Ni(II), Co(II) and Zn(II). When introducing metals with different oxidation states, however, no competitive behavior for the montmorillonite surface could be detected. For example Co(II) or Zn(II) at different concentrations was not found to affect the sorption of Eu(III), suggesting that sorption competition is selective and that different surface sites are responsible for the uptake of metal ions with different chemistries. In agreement with the study by Bradbury and Baeyens, Trivedi et al. [4] observed the competition between Ni(II) and Zn(II) on goethite at pH 5–7 when the total metal ion concentration was close to surface site saturation. At lower metal concentrations, when the goethite sorption sites were not fully occupied, no competition was found between both metals. This implies that at least the sorption of Ni(II) and Zn(II) is taking place on the same goethite surface sites. Also Heidmann et al. [5] observed a decrease in the Cu(II) uptake by illite in the presence of Pb(II). A similar observation was done by Christl and Kretzschmar [6], who showed that Pb(II) reduces the sorption of Cu(II) on hematite. However, interestingly the effect of Cu(II) on Pb(II) adsorption was not equally strong, suggesting that there could be other factors influencing sorption competition of metals than the oxidation state alone. A study by Soltermann et al. [7] investigating the competitive uptake of Fe(II) and Zn(II) by montmorillonite also contradicts the theory of Bradbury and Baeyens. Soltermann et al. [7] found that Fe(II) influences the sorption of Zn(II) in the trace concentration range, while Zn (II) has no influence at all on Fe(II) despite their identical oxidation states. The lack of competition was explained by the oxidation of Fe(II) to Fe(III), that has a higher affinity towards the surface sorption sites on montmorillonite compared to Zn(II). This hypothesis of Soltermann et al. [7] would imply that metals with stronger complexation strengths for solid surfaces would be able to take over or block some of the surface sites from the metal that is more weakly complexed onto the surface. However, competition between metals with different complexation strengths does not agree with the results obtained by Bradbury and Baeyens [3], implying that the uptake behavior of metals in the presence of competing elements is rather intricate and in general not a very well understood process.

In the present study sorption competition on the aluminum oxide mineral corundum has been investigated from the perspective of the relatively mobile pentavalent Np(V) ion in the presence of trivalent lanthanide (Ln) ions Eu(III) and Gd(III), taken as analogues for the trivalent actinides Pu(III), Am(III), and Cm(III). Neptunium is a relevant radionuclide to be considered in safety assessments of the final disposal of SNF. Because of its long half-life (2.144×10^6 years), ^{237}Np will be one of the most important dose affecting radionuclides in SNF after 1×10^5 years [8]. Under reducing final disposal conditions, Np is expected to exist as poorly soluble Np(IV) in the nuclear waste matrix. In contact with oxic groundwater, however, Np may be oxidized to Np(V) with a significantly higher solubility in comparison to other actinides.

The trivalent actinides are rather soluble (depending on pH), but they show a strong complexation for solid surfaces in the circumneutral to alkaline pH range (e.g. [9–12]), which reduces their mobility in the geosphere. The general tendency for hydrolysis and complex formation of actinides follows the order $An^{4+} > AnO_2^{2+} > An^{3+} > AnO_2^{+}$ [13,14]. Furthermore, the strength of hydrolysis of the sorbing metal has been shown to directly affect the surface complexation strength: a linear correlation between the aqueous hydroxide species of various actinides and their corresponding surface complexation constants has been observed in e.g. Bradbury and Baeyens [2], for montmorillonite and in Dzombak and Morel [15], for hydrous ferric oxides. Thus, we expect that trivalent lanthanide analogues used in the present study would form stronger surface complexes on corundum in comparison to Np(V), and therefore to possibly influence the complexation of Np(V) on the mineral surface. Corundum (α-Al_2O_3) was chosen for this study since the surface structure of the oxide is relatively simple and well characterized, consisting of Al–OH groups that act as sorption sites for the actinides.

To account for potential sorption competition reactions between Np(V) and Ln(III) in the present study, the macroscopic Np(V) sorption behavior on corundum as a function of pH (pH-edges) and Np(V) concentration (isotherms) has been investigated both in the absence and presence of competing Eu(III). Surface complexation modelling (SCM) has been applied to the batch sorption data to obtain surface complexation constants for Np(V) on corundum and to help interpreting the experimental batch sorption data. To shed light on microscopic sorption processes, such as changes in the Np(V) surface speciation or its coordination geometry in the presence/absence of Ln(III), X-ray absorption spectroscopy (XAS) was performed on the samples containing Np(V) with and without Gd(III) as a representative of Ln(III).

2. Materials and methods

2.1. Corundum characterization

Commercially available corundum, α-Al_2O_3 (from Taimei Chemicals, Tokyo, Japan, Taimicron TM-DAR) was used in the experiments. X-ray powder diffraction (XRD) analysis using the PANalytical X'Pert PRO multipurpose X-ray diffractometer confirmed the material to be alpha phase corundum and no impurities were found. The specific surface area of the mineral has previously been determined to be 14.5 m^2/g with the N_2-BET technique [12]. The particle size and shape of the material was determined with field emission scanning electron microscope (FESEM). The spherical particles showed a homogenous particle size distribution with the size ranging from 100 nm to 200 nm. The isoelectric point (IEP), i.e. the pH value where the electrokinetic charge of the surface is zero, of the corundum particles was determined by measuring the ξ-potential (Malvern Zetasizer Nano) of the mineral as a function of pH. The ξ-potentials were measured in three different

solutions; MilliQ-water, 0.01 M $NaClO_4$ and 0.1 M $NaClO_4$ using a mineral concentration of 1.0 g/l. The IEP of the corundum was found to be at pH 9.7 (see supporting information Fig. SI1). The potentiometric titrations were carried out by Metrohm 907 Titrando. The additions of 5 mM acid solution were done in small increments controlled by a Metrohm software and the pH was measured two minutes after addition of titrant. The titration was started from a basic starting pH and the initial suspension in 0.01 M $NaClO_4$ was equilibrated overnight under humidified argon. During the titration a stream of humidified argon was flowing over the suspension to minimize intrusion of carbon dioxide. Initial solid content was 9.6 g/l in 50 ml of electrolyte solution. The relative surface charge density σ (C/m^2) was calculated from the raw data by subtracting the blank. The independently measured isoelectric point was used to transfer the relative to absolute surface charge densities. The surface titration data were fitted using Diffuse Double-Layer model, see supporting information for more details.

It is well known, that the surface of aluminum oxides can change during the hydration process when mineral is contacted with aqueous solutions [16]. Thus, the corundum suspension was always freshly prepared from dry powder for batch experiments to avoid unnecessary aging of the mineral suspension and modifications of the surface. In the surface complexation modelling (discussed later in the text) the surface of corundum is considered to consist of Al–OH groups that protonate or deprotonate, depending of the pH.

2.2. Chemicals

All sorption and speciation investigations were performed in a glove box, under nitrogen atmosphere, to exclude the formation of metal-carbonato-complexes on the mineral surface or in solution that could affect the uptake of the metals by the corundum mineral. The neptunium experiments were performed with a ^{237}Np-tracer that was confirmed to be Np(V) by UV–VIS prior to the experiments. The europium stock solution used in the batch sorption investigations was either prepared by dissolving $EuCl_3 \times 6\ H_2O$ in 0.01 M $HClO_4$, or by diluting a commercial Eu 1000 ppm standard to the desired concentration. The gadolinium stock solution for XAS measurements was prepared from $GdCl_3 \times 6\ H_2O$ similarly to the Eu(III) stock solution. TRIS (tris(hydroxymethyl) aminomethane) and CHES (N-Cyclohexyl-2-aminoethanesulfonic acid) buffers (concentration 0.01 M) were used in isotherm and kinetic experiments to stabilize the suspension pH at pH 8 and pH 9, respectively. Buffers were not found to affect the metal ion complexation. All the experiments were performed in 10 mM $NaClO_4$ solutions and NaOH and $HClO_4$ were used for pH adjustments. All chemicals were carbonate free and at least of analytical grade.

2.3. Batch sorption experiments

The experimental conditions in terms of mineral concentration from 0.5 g/l to 5.0 g/l and equilibration time from 1 to 14 days were optimized by investigating the uptake of 10^{-6} M Np(V) and Eu(III) as a function of corundum concentration or as a function of equilibration time, respectively, at a constant pH of 8 in 0.01 M $NaClO_4$. Based on these investigations the pH-dependent Np(V) uptake experiments and the Np(V) isotherm experiments as a function of Np(V) concentration in the absence and presence of Eu(III) as competing metal were performed at two solid concentrations of 0.5 g/l and 5 g/l using an equilibration time of one week, as will be explained later.

The pH-dependent sorption investigations in the absence of Eu (III) were performed with initial Np(V) concentrations of 1×10^{-9} M, 1×10^{-6} M and 1×10^{-5} M in 0.01 M $NaClO_4$. After Np(V) addition to the corundum suspension the pH was adjusted within the pH-range 3–12 using 0.01–0.1 M $HClO_4$ or NaOH. The samples containing the competing metal Eu (1×10^{-5} M) were prepared by adding Eu(III) to the corundum suspension in a first step at low pH, followed by pH adjustment of the samples to the desired pH-value (slow increase of pH to avoid precipitation). After an equilibration time of 2 days 10^{-9} M or 10^{-6} M Np(V) was added to the samples and the pH was readjusted to correspond to the values before Np(V) addition. After equilibration (one week), the phase separation was done by centrifugation, either with an ultracentrifuge at 90,000 rpm or at 6,000 rpm for one hour and the supernatant was used for measuring aqueous Np(V) and Eu (III) concentrations. Np isotherms were done in TRIS or CHES-buffered solutions at approximately pH 8 and 9. Isotherm samples were prepared similarly to the pH-edge samples described above, except the initial Np concentration was varied between 2.5×10^{-10} M and 5×10^{-6} M.

Inductively coupled plasma-mass spectrometry (ICP-MS) was used for determination of the low concentration Np samples and liquid scintillation counting (LSC) was used for the samples with higher concentration. The concentrations of Eu and Gd were determined from the supernatants by ICP-MS.

2.4. X-ray absorption spectroscopy - sample preparation and measurements

For XAS measurements, Gd(III) was employed as a competing Ln (III) instead of Eu(III), in order to avoid potential reduction of Eu(III) to Eu(II) by the strong irradiation of synchrotron X-rays. Two corundum (5.0 g/l) suspension samples were prepared in 240 ml. In the first sample an initial Gd concentration of 2×10^{-5} M was added to the mineral suspension. To avoid precipitation of Gd $(OH)_3$ from oversaturated solutions when increasing the pH of the suspension, the pH adjustment was done very slowly over several days until the desired pH of 9 was reached. Thereafter, the sample was equilibrated for one day before addition of 2×10^{-5} M Np and the pH was readjusted to 9. As discussed later, the batch experiment showed that the sorption of 1×10^{-5} M Np (V) is significant only above pH 8.5, thus pH 9 was chosen for XAS samples to ensure the sufficient sorption of Np(V) onto the mineral surface. In the second sample, an initial Np concentration of 4×10^{-5} M was used and the pH of the suspension was adjusted to pH 9. After Np addition, both samples were equilibrated in a shaker for at least two days before centrifugation at 6,000 rpm. The supernatant was decanted and the samples were placed in Teflon sample holders as a wet paste, which were sealed in the N_2-glove box, frozen, and stored in liquid nitrogen until the measurement. The equilibrium concentrations of Np and Gd in the solutions were determined by LSC and ICP-MS, respectively. Around 100% of initial Gd(III) and 74% of Np(V) were adsorbed at the corundum surface which corresponds to surface loadings of 700 mg/kg or 1,400 mg/kg of Np and 480 mg/kg of Gd.

XAS measurements were conducted at the Rossendorf beamline (ROBL) at the European Synchrotron Radiation Facility (ESRF) in Grenoble, France. X-ray absorption spectra including both X-ray absorption near-edge structure (XANES) and extended X-ray absorption fine structure (EXAFS) regions were recorded at the Np L_{III}-edge (17,610 eV) under dedicated ring operating conditions of 6 GeV and 150–200 mA. A Si(1 1 1) double-crystal monochromator was used to monochromatize the incoming synchrotron X-rays. The fluorescence spectra were collected with a 13-element Ge solid state detector (Canberra) and ionization chambers. The measurements were performed at 15 K with a cryostat in order to reduce thermal noise and to avoid the radiation-induced reduction of neptunium during the measurements. Energy calibration of the

collected spectra was performed by the simultaneous measurement of the absorption spectrum of yttrium foil (Y K-edge defined as 17,038 eV). A minimum of four spectra were collected for each sample, and the spectra were averaged for data analysis according to standard procedures [17] with the software WinXAS, version 3.2 [18]. The threshold energy, $E_{k=0}$, was defined as the first inflection point of the Np L_{III}-edge absorption edge. Theoretical fitting of the extracted EXAFS spectra was performed both in the *k*- and *R*-spaces. EXAFS theoretical phase and amplitude functions were calculated by using the *ab-initio* code FEFF 8.20 [19]. The amplitude reduction factor, S_0^2, was fixed at 0.9, while the shifts in energy threshold, ΔE_0, were varied but constrained to be the same value for all the shells. Detailed descriptions of EXAFS structure parameters can be found in e.g. Bunker [20] and Newville [21]. For the FEFF calculations a hypothetical structure of a Np(V) edge-sharing sorption complex [22] was used.

2.5. Surface complexation modelling

Surface complexation modelling (SCM) of Np sorption on corundum was based on the batch sorption results. For the fitting of the data we applied the experimentally determined specific surface area (14.5 m^2/g [12]), surface protolysis constants determined by potentiometric titrations within the Diffuse Double-Layer model (DLM). For the surface site density we used the value recommended by Davis and Kent [23], i.e. 2.31 nm^{-2}. The selected model is implemented in various geochemical codes. The modelling was performed with PHREEQC version 3.1.7 [24] coupled with the parameter estimation software UCODE 2005 [25]. Thermodynamic parameters for aqueous speciation were taken from the NEA TDB including its update [26,27].

3. Results and discussion

3.1. Batch sorption investigations

3.1.1. Effect of solid/liquid ratio and the equilibration time on Eu(III) and Np(V) sorption

Np sorption at three different mineral concentrations, 0.5, 2.0 and 5.0 g/l was studied at pH 8. Uptake of Np increased from 24% to 76% with increasing mineral concentration, resulting in an average $\log K_d$ of 2.76 ± 0.05 l/kg. For further batch sorption experiments, corundum concentrations of 0.5 g/l and 5.0 g/l were chosen. Eu sorption at varying mineral concentration could not be accurately determined, due to the exceeding of the analytical detection limits at pH 8 where (almost) quantitative sorption occurs.

To estimate the surface saturation for the chosen mineral concentrations and at different metal ion concentrations, we used a site density value of 2.31 nm^{-2}, recommended by Davis and Kent [23]. This value is an estimation that represents the surface sites which can be protonated and be used for cation binding. Using this approximation and assuming a monodentate complexation, we achieve surface saturation of 36% and 3.6% for 1×10^{-5} M Eu on 0.5 g/l and 5.0 g/l corundum, respectively. For 1×10^{-5} M Eu + 1×10^{-6} M Np, corresponding to a total metal concentration of 1.1×10^{-5} M, we get surface loadings of 40% and 4% for 0.5 g/l and 5.0 g/l corundum, respectively. Hence, at the higher mineral concentration, 5.0 g/l, mineral surface sites are considered to be sufficient and competitive sorption effects are less likely to happen. However, at the lower mineral concentration, 0.5 g/l, the surface loading is already substantial, and competition could occur.

Eu and Np sorption kinetics were tested by studying the sorption percentages of metals at different contact times with corundum at pH 8 (see supporting information Fig. SI3). Equilibration time of one week was found to be sufficient for both Eu and Np to reach a steady-state in the batch experiments.

3.1.2. Sorption of Np(V) on corundum as a function of pH

In the batch sorption experiments the uptake of Np as a function of pH shifts to higher pH values when increasing the initial Np concentration from 1×10^{-9} mol/l to 1×10^{-5} mol/l (Fig. 1). The pH at 50% Np sorption ($pH_{50\%}$) for 1×10^{-9}, 1×10^{-6} and 1×10^{-5} mol/l Np is at pH 6.9, 7.6 and 8.3, respectively. According to Dzombak and Morel [15] and Davis and Kent [23] this kind of pH-edge shift is linked to either saturation of available sorption sites, steric/electrostatic effects, where the attached metal exerts a repulsive force on metal ions remaining in solution, or due to heterogeneity of the surface binding sites, i.e. the presence of multiple site types on the mineral surface. A similar shift in the Np pH-edge would be expected if the competing metal added to the system is bound to the same surface sites, or if these surface sites are (partially) blocked by electrostatic effects caused by other attached metal cations on the surface. However, if the competing metal is binding more weakly compared to the other metal or if both metals are binding on different sites, adsorption of the competing metal has only a minor effect on the position of the pH-edge [1]. Thus, based on these facts, in case Eu occupies the same sorption sites as Np, we should see a shift in the Np pH-edge position when adding 1×10^{-5} mol/l Eu before 1×10^{-9} mol/l Np. Fig. 1 shows that for Np this shift is considerable when Np concentration is increased ($pH_{50\%}$ 6.9 for 1×10^{-9} mol/l Np, compared to $pH_{50\%}$ 8.3 for 1×10^{-5} mol/l Np). Conversely competitive sorption experiments performed by adding 1×10^{-5} mol/l Eu to the suspension two days before the addition of 1×10^{-9} mol/l or 1×10^{-6}

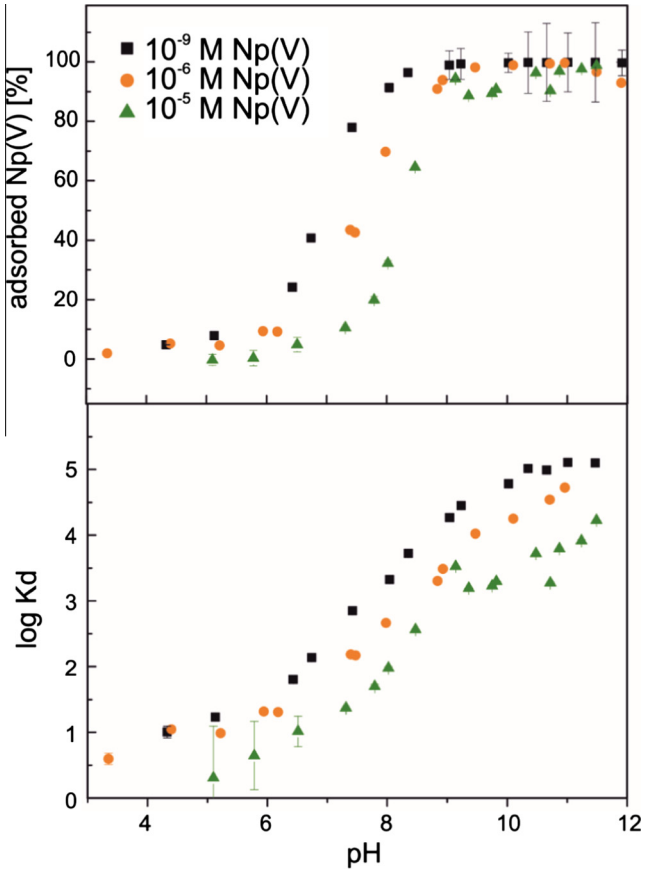

Fig. 1. Sorption of 1×10^{-9}, 1×10^{-6} and 1×10^{-5} mol/l Np on 5.0 g/l corundum as a function of pH in 0.01 M $NaClO_4$.

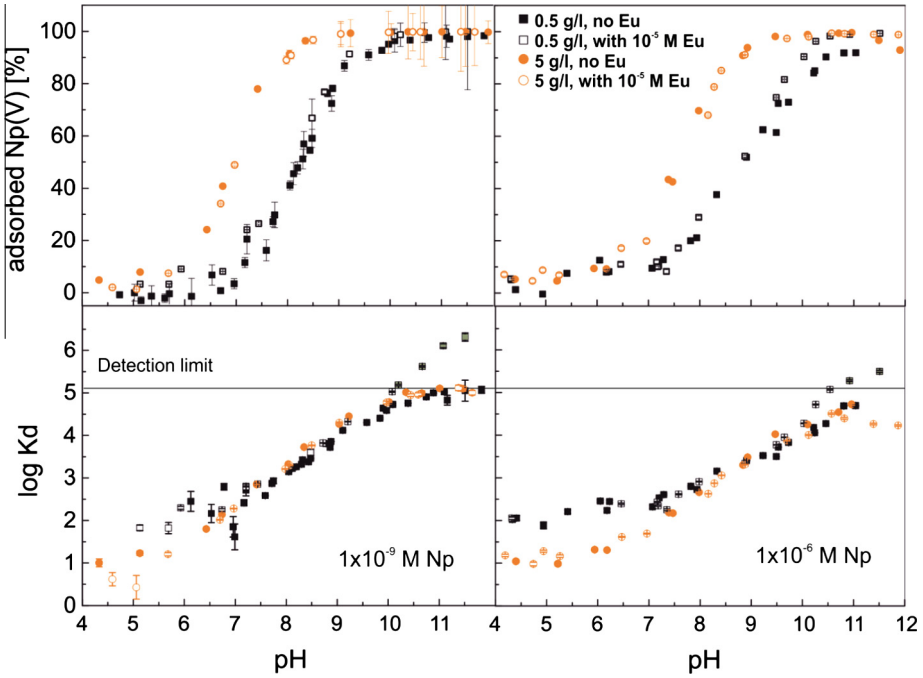

Fig. 2. Sorption of 1×10^{-9} mol/l (left) and 1×10^{-6} mol/l (right) Np on 0.5 g/l and 5.0 g/l corundum with and without 1×10^{-5} mol/l Eu added to the solution prior to Np addition.

mol/l Np (Fig. 2) show no change in the pH-edge position, and, therefore no indication of a significant competition between Eu and Np. This implies that Eu(III) and Np(V) are occupying different sites on the corundum surface, since there is no noticeable competition even when more strongly sorbing Eu is allowed to occupy the preferred surface sites before introducing Np to the suspension.

3.1.3. Sorption of Np(V) on corundum as a function of Np(V) concentration

Investigating the sorption competition between Np and Eu at varying Np concentrations and constant Eu concentration provides information on potential competitive effects taking place at specific site types e.g. so called strong sites that are high affinity sites with low abundance [2]. Bradbury and Baeyens [3] showed that sorption competition of metals was mainly visible at a trace concentration level of the index metal together with a high concentration of the blocking metal (i.e. competing metal), since this is the area where strong sites prevail. Following this idea, we investigated the effect of concentration on the sorption competition by varying the Np concentration at fixed Eu concentration and constant pH and compared these results with Np sorption in the absence of Eu. In these experiments the initial Eu concentration (1×10^{-5} M) was relatively high compared to initial Np concentration (2.5×10^{-10}–5×10^{-6} M). Isotherms were performed at pH ~ 8 and ~9 for both mineral concentrations of 0.5 g/l and 5.0 g/l (Fig. 3). Isotherms for two mineral concentrations were plotted in separate figures (Fig. 3, left and right), however, this was done only for clarification, and the mineral concentration did not affect the result.

Generally the shape of the isotherm may denote the number of different surface site types taking part in the sorption process. Np was found to behave ideally at low initial concentrations, where the slope of the isotherm is one and only at higher concentrations the slope is less than one. This might be explained either by saturation/electrostatic effects at higher surface loadings or, alternatively, non-linear sorption isotherms could also indicate the existence of at least two different site types with different affinities towards sorbing metals. Often these different site types are referred to as strong and weak sites. Strong sites have high sorption affinity but low abundance compared to weak sites that have high capacity but low sorption affinity, and, therefore, strong sites can be regarded as responsible for metal sorption onto mineral

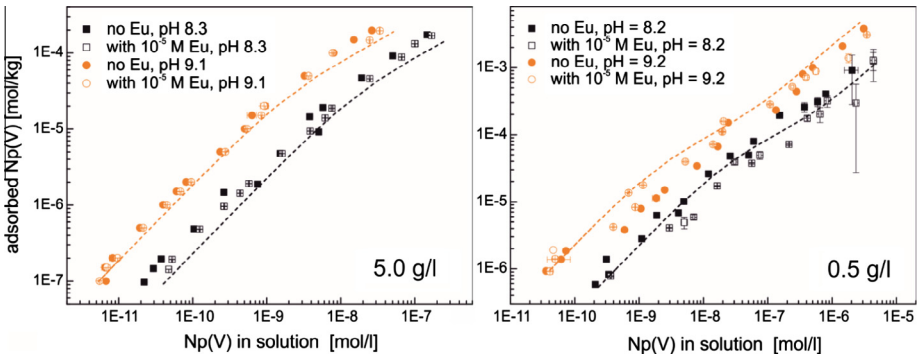

Fig. 3. Sorption isotherms of Np on 5 g/l (left) and 0.5 g/l (right) corundum with (open symbols) and without (closed symbols) 1×10^{-5} mol/l Eu added to the solution prior to Np addition at pH 8 and 9. Dashed line: sorption complexation modelling.

surfaces at trace concentrations [28,29]. When strong sites are saturated, weak sites become operative. If sorption competition occurs, a significant effect would be expected mainly at the concentration region where strong sites are important, i.e. at trace Np concentrations, as discussed in the previous section. Since there are no signs of competition even at high Np concentrations, where both strong and weak sites should be active, we exclude any sorption competition effects of Eu(III) on Np(V) sorption at different site types. One of the reasons why corundum was chosen for this study is the simplicity of its structure (see SI for more information), and the existence of Al–OH surface groups that are also present on the surface of more complex aluminosilicates. However, aluminosilicates, such as some clay minerals, with permanent negatively charged surface planes (such as montmorillonite, illite and biotite), might show different results for competitive sorption of metals. The permanent structural charge also allows for cation exchange at low pH, which should be favored by trivalent metals over NpO_2^+ due to the higher positive charge, and this difference needs to be taken into account if these results are extended to more complex surfaces.

3.2. Np(V) surface complexation modelling investigations

A bidentate inner-sphere surface complex of Np(V) on corundum, spectroscopically identified in this study (see discussion later in the text) was used as a basis for our surface complexation model. Aluminol groups were treated as independent Al–OH groups. For the fitting of the experimental pH-edge batch sorption data with a solid/liquid ratio of 0.5 g/l and 5 g/l corundum and with Np concentrations of 10^{-9}, 10^{-6} and 10^{-5} M in 0.01 M $NaClO_4$ solution, it was necessary to include the concept of strong and weak binding sites as used by Dzombak and Morel [15]. The ratio of strong binding sites was varied between 0.1 and 2% of total available sites. The best fit was obtained for 0.5% strong (≡(s)AlOH) and 99.5% weak binding sites (≡(w)AlOH). Thus, two log$K$ values have been obtained for the formation of the bidentate inner-sphere surface complex (Eq. (1)). Aqueous complexation of Np(V) in CO_2-free conditions is discussed in detail in the supporting information. In Eq. (1) only one of the two surface hydroxyl group involved in the Np surface sorbed complex is assumed to be deprotonated. However, modelling was also tested for a Np bidentate complex with two deprotonated surface hydroxyl groups and release of two protons (Fig. SI 6), resulting in a too steep pH dependent uptake (at least at low metal ion concentrations where only strong sites are involved).

$$2 \equiv (s/w)AlOH + NpO_2^+ + 3H_2O \leftrightarrow ((\equiv (s/w)AlO)_2H)NpO_2(H_2O)_3 + H^+ \quad (1)$$

For comparison, we also considered modelling with monodentate inner-sphere surface complexes (Eq. (2)), since it is widely used in literature for Np sorption on aluminum and iron oxides [30–32]. However, our spectroscopic investigations do not support the formation of such monodentate complexes.

$$\equiv (s/w)AlOH + NpO_2^+ + 4H_2O \leftrightarrow (\equiv (s/w)AlO)NpO_2(H_2O)_4 + H^+ \quad (2)$$

Modelling was performed with the protolysis constants obtained by potentiometric titrations. The protolysis constants ($pK_1 = 6.85$, $pK_2 = -12.43$) give a calculated IEP of 9.64, which is consistent with our experimentally determined IEP of 9.7 (see supporting information). The equilibrium constants (logK° values) for surface complexation reactions for Np obtained by surface complexation modelling in this work are given in Table 1 and all the fitting curves for the pH-edges are presented in supporting information (Figs. SI 4–6). Modelling was tested for the isotherm data, presented in Fig. 3, for the bidentate inner-sphere surface complex with one deprotonated surface hydroxyl group, since this model produced the best fit for pH-edge data. The obtained model predicts reasonably well the uptake of Np at lower as well as higher metal concentrations.

Table 1
Surface reactions for Np(V) surface complexation modelling and optimized equilibrium constants.

Reaction	logK°
≡(s/w)AlOH + H^+ ↔ ≡(s/w)$AlOH_2^+$	6.85
≡(s/w)AlOH ↔ ≡(s/w)AlO^- + H^+	−12.43
2≡(s)AlOH + NpO_2^+ + 3 H_2O ↔ ((≡(s)AlO)$_2$H) $NpO_2(H_2O)_3$ + H^+	−0.97
2≡(w)AlOH + NpO_2^+ + 3 H_2O ↔ ((≡(w)AlO)$_2$H)$NpO_2(H_2O)_3$ + H^+	−4.21
≡(s)AlOH + NpO_2^+ + 4 H_2O ↔ ≡(s)$AlONpO_2(H_2O)_4$ + H^+	−1.33
≡(w)AlOH + NpO_2^+ + 4 H_2O ↔ ≡(w)$AlONpO_2(H_2O)_4$ + H	−4.67

The ratio of strong and weak sorption sites (0.5 and 99.5%) is in agreement with the earlier studies for iron oxide goethite [33]. The sorption of Np(V) as a bidentate inner-sphere complex onto corundum was also studied by Wang et al. [34]. Although they use a bidentate inner-sphere surface complex, their model cannot explain the shift of the experimentally obtained data points with the solid-liquid ratio and the Np(V) concentration (see Fig. SI 7). Wang et al. [34] also published models for the sorption of Np(V) onto other aluminum-containing mineral phases than corundum, γ-Al_2O_3, boehmite (γ-AlOOH) and gibbsite (γ-$Al(OH)_3$) but only for corundum, a bidentate complex was assumed.

The suggested model, with bidentate Np surface complex with one proton released from the surface, combines robustness, which results from a wide range of experimental data, with a realistic chemical speciation obtained by spectroscopic studies. However, the fit of the used DLM to the experimental sorption data and to the potentiometric titrations is not excellent, and a more complex model might be needed to obtain a better fit for the experimental results. The monodentate inner-sphere surface complex model also resulted in a relatively good fit, but our spectroscopic results do not support the formation of Np-monodentate complexes.

3.3. X-ray absorption spectroscopy and coordination geometry of Np(V) on corundum

The k^3-weighted Np L_{III}-edge EXAFS spectra of the corundum samples and their corresponding Fourier transforms (FTs) are presented in Fig. 4. A summary of the obtained EXAFS structural parameters is given in Table 2. A complete table of all the EXAFS structural parameters obtained from theoretical fitting is provided in Table SI 1 in the supporting information.

The noise level of the acquired EXAFS data was estimated by checking the FT peak magnitude at the longer R range between 15 and 20 Å of the FT spectrum, as only random fluctuations are expected in this longer R range and, hence, no significant signal should be detectable (Fig. SI8) [35]. This means that only the peaks above this noise level could be considered as meaningful signals to acquire structural information.

For the theoretical fitting of the acquired EXAFS data, a bidentate edge-sharing (ES) Np(V) complex (Fig. 5) was presumed, in analogy with the precedent studies by Elo et al. [36] and Gückel et al. [22]. We used similar input parameters for the fitting of our sample spectra as previously used in Elo et al. [36], investigating the sorption of 2×10^{-5} M Np(V) on 5 g/l of the identical corundum mineral supplied by Taimei Chemicals, Tokyo, Japan, Taimicron TM-DAR. The bond distances of Np–O_{ax} and Np–O_{eq} calculated for our present samples containing 4×10^{-5} M Np(V) are in good agreement with those reported by Elo et al. [36] (Table SI 1).

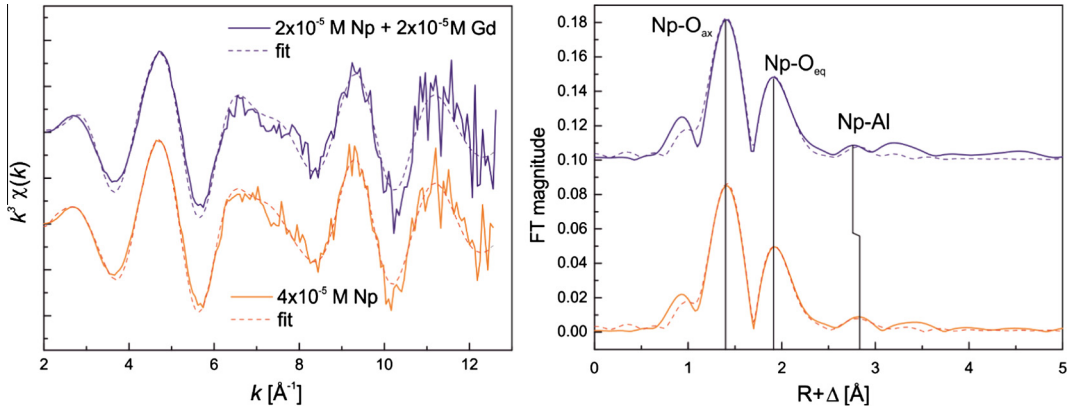

Fig. 4. k^3-weighted Np L_{III}-edge EXAFS spectra (left) and corresponding Fourier transforms (right) of corundum samples containing 4×10^{-5} M Np or 2×10^{-5} M Np and 2×10^{-5} M Gd at pH 9. Solid lines; experimental data, dashed lines; theoretical fitting. Phase shifts (Δ) are not corrected in the FTs.

Table 2
EXAFS structural parameters obtained for Np(V) sorbed on corundum. CN = coordination number, R = interatomic distance between the Np center and neighboring atoms, σ^2 = Debye-Waller factor (i.e. thermal disorder of the scattered atoms), ΔE_0 = shift in threshold energy, S_0^2 = amplitude reduction factor, $R_{\%}$ = fitting residual.

Sample	Shell	CN	R (Å)	σ^2 (Å^2)	ΔE_0 (eV)	S_0^2	$R_{\%}$ (%)
4×10^{-5} M Np	Np–O_{ax}	2.0[a]	1.86	0.0018	4.96	0.9[a]	7.0
	Np–O_{eq}	4.5	2.50	0.0075			
	Np–Al	1.66	3.39	0.012			
2×10^{-5} M Np + 2×10^{-5} M Gd	Np–O_{ax}	2.0[a]	1.86	0.0023	4.60	0.9[a]	12.3
	Np–O_{eq}	4.3	2.49	0.0072			
	Np–Al	1.6	3.30	0.015			

[a] Fixed parameters.

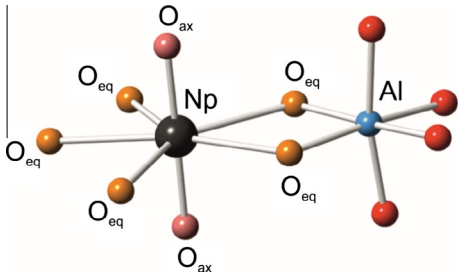

Fig. 5. Suggested structure of the Np surface edge-sharing complex on corundum surface adapted from Gückel et al. [22].

The Np–O_{ax} and Np–O_{eq} distances of our samples are also well comparable to the values reported by Gückel et al. [22] for a bidentate edge-sharing sorption complex of Np(V) on gibbsite at pH 7.5, where the Np–O_{ax} and Np–O_{eq} distances are 1.84 Å and 2.46 Å, respectively. The weak but significant signal at $R + \Delta = 2.5$–2.7 Å (Fig. 4) can be assigned to the Np–Al single scattering (SS) path [36], while another peak at around $R + \Delta = 3.2$ Å could be assigned to multiple scattering (MS) paths of the linear O_{ax}–Np–O_{ax} arrangement [37]. Both paths were included in the fitting of the two Np(V) containing samples. The Np–Al distances determined in our samples (3.30 and 3.39 Å) are comparable to that obtained by Elo et al. [36] (3.38 Å), but significantly shorter than that reported for Np(V) sorbed on gibbsite (3.48 Å) [22]. This suggests that our data can be reasonably fitted by assuming the coordination geometry of a bidentate ES complex and that the speciation of Np(V) remains unchanged even though the metal ion concentration has been doubled in comparison to the precedent study by Elo et al. [36]. When comparing our samples in the absence and presence of Gd(III), the Np–Al distances show a contraction from 3.39 Å to 3.30 Å, while the Np–O_{ax} and Np–O_{eq} distances remain unchanged. Furthermore, our EXAFS-FT spectra show an additional peak at $R + \Delta = 3.2$ Å in the presence of Gd(III), which is not possible to reproduce completely only by assuming the MS paths of the neptunyl(V) arrangement [37]. These facts indicate that the presence of Gd(III) causes some changes in the Np(V) speciation and its coordination geometry. The EXAFS-FT peak appeared at $R + \Delta = 3.2$ Å for the Np(V) + Gd(III) sample could possibly arise from e.g. (1) the scattering from heavy atoms, such as Gd(III) or, (2) other Np–Al arrangements which have longer Np–Al distances than the ES arrangement. The appearance of a Np(V)–Gd(III) peak due to closely located metal surface complexes on the corundum surface is unlikely due to the relatively low amount of metal ions on the corundum surface capable of saturating only 14% of available surface sites. Due to the rather high concentration of the trivalent lanthanide in combination with the high pH required for sufficient Np (V) sorption in the XAS samples, $Gd(OH)_3$ and/or $Al,Gd(OH)_3$ could potentially precipitate on the corundum surface from oversaturated solutions prior to the adsorption of Np(V). This could account for the formation of other types of Np(V) sorption species which would explain the EXAFS-FT peak $R + \Delta = 3.2$ Å for the Np(V) + Gd(III). The fitting of such a Np(V) complex, however, did not provide a satisfactory reproduction for our EXAFS data (see supporting information for more discussion). Thus, further investigation is required to interpret this peak.

EXAFS data for Np adsorbed on oxide minerals are scarce, making it difficult to assess our data to confirm whether or not a surface complex, other than the bidentate edge-sharing one, could be expected on the corundum surface. Müller et al. [38] investigated Np(V) sorption onto the iron oxide mineral hematite, and identified at least one binary edge-sharing Np(V) complex on the surface with a Np–Fe distance of 3.70–3.73 Å. A fit including a second Np–Fe peak at shorter distances (3.47 Å) was also considered. However, this model resulted in a change of the coordination number (CN) from 1.3 to 1.9 of the Np–Fe complex at longer distances which could be connected to a double corner-sharing (DCS) complex with a CN of 2. In the paper by Gückel et al. [22] investigating Np(V) sorption on gibbsite, only one Np(V) complex, corresponding to the bidentate ES complex, has been identified. However, compared to the surface loading of Np(V) in our samples, Gûckel et al. [22] used relatively low surface loading (139 mg/kg) of Np (V) and it is unlikely that Np(V) could be sorbed via different geometries with such a low surface loading. Arai et al. [39] studied the Np(V)-carbonate sorption on hematite and suggested Np(V) ternary inner-sphere complexation via ES configuration, together with outer-sphere complexation. There is no spectroscopic data

for Np(V) complexation at a higher concentration range where more than one surface configuration could be expected for surface sorbed Np(V). For uranyl(VI) (UO_2^{2+}), two different complexes have been identified on gibbsite (α-$Al(OH)_3$), a DCS and an ES inner-sphere complexes [40]. The DCS complex might be further away from the surface compared to ES complex, which is supported by DFT-calculations for U(VI) sorption on goethite (α-FeOOH) [41]. The attachment of Np(V) to the surface with more than one geometry might explain the differences between the two samples in this study. However, with the very limited amount of data, additional XAS investigations need to be performed to verify the proposed influence of Gd(III) on the Np(V) sorption speciation.

4. Conclusions

The aim of this work was to study the sorption competition between metals with different chemical characters. The question was: could a trivalent metal, that is presumed to attach more strongly onto the Al–OH groups of corundum, hinder or affect the sorption of neptunium? Earlier studies on sorption competition have showed competition between metals with similar chemistries, i.e. hydrolysis properties and charge, but they have not taken a closer look into the possible sorption competition between metals with dissimilar chemistries. In this work, we have combined batch experiments with spectroscopic studies to give a comprehensive picture about the sorption of Np(V) in the absence and presence of competing trivalent metals.

In the absence of the competing trivalent lanthanide element (Eu(III) or Gd(III)) we found that depending on the initial Np(V) concentration, sorption of 10^{-9} M Np on 5.0 g/l mineral starts already at around pH 6, whereas for 10^{-5} M Np sorption starts at around pH 7.5. This shift can be explained by the fact that the higher concentration is already outside of the ideal concentration range of Np, where the K_d is constant. With the isotherm experiments at constant pH of 8 and 9, we found that at low Np concentrations the sorption of Np is independent of the initial concentration and K_d remains stable. Only at higher Np concentrations a decrease in sorption is observed, which might be caused by the presence of different site types or saturation/electrostatic effects taking place at increasing surface loadings. The addition of the competing Ln(III) to the mineral suspension did not result in any visible changes in the Np(V) uptake by corundum in the pH-edge and isotherm experiments, suggesting that these metals do use different sites upon sorption. The XAS measurements indicate the presence of binary bidentate edge-sharing Np(V) complexes (ES) in the absence of competing Ln(III). In the presence of Gd (III), the Np–Al distance contracts from 3.39 Å to 3.30 Å and an additional peak appears at $R + \Delta = 3.2$ Å. This could indicate that Np(V) is attaching to the surface in different geometries, e.g. edge-sharing and double corner-sharing (DCS) configurations. However, further detailed investigation is required to verify this hypothesis.

Surface complexation modelling using the Diffuse Double-Layer model was applied to the batch experiments. We included the concept of strong and weak binding sites in the modelling and the best fit was obtained for 0.5% strong (≡(s)AlOH) and 99.5% weak binding sites (≡(w)AlOH). We obtained log K for the Np(V) sorption as a bidentate inner-sphere surface complex with one exchangeable proton on strong and weak sites resulting in an improved model for Np(V) uptake by corundum.

This study shows that the concept of competitive sorption is not easily understandable and more research concerning the competition between metals with different or similar chemistries is required. Furthermore, simple batch experiments do not necessarily reveal the possible changes occurring on a molecular scale, such as changes in the complex structure or metal ion speciation. Thus, sorption competition research should, when possible, be accompanied by spectroscopic methods.

Acknowledgements

The authors would like to thank Dr. Marianne Kemell for FE-SEM measurements, Dr. Mikko Heikkilä for XRD measurements of the mineral and Dr. Juhani Virkanen for help with the ICP-MS measurements. Stephan Weiß is thanked for assistance in preparing XAS samples. The ROBL staff is greatly acknowledged for their help and support during the XAS measurements. The Finnish Doctoral Programs for Nuclear Engineering and Radiochemistry (YTERA) and Chemistry and Molecular Sciences (CHEMS) are thanked for financial support for this work.

Appendix A. Supplementary material

Supplementary data associated with this article can be found, in the online version, at http://dx.doi.org/10.1016/j.jcis.2016.08.035.

References

[1] M.M. Benjamin, J.O. Leckie, Competitive adsorption of Cd, Cu, Zn, and Pb on amorphous iron oxyhydroxide, J. Colloid Interface Sci. 83 (2) (1981).
[2] M.H. Bradbury, B. Baeyens, Modelling the sorption of Mn(II), Co(II), Ni(II), Zn (II), Cd(II), Eu(III), Am(III), Sn(IV), Th(IV), Np(V) and U(VI) on montmorillonite: linear free energy relationships and estimates of surface binding constants for some selected heavy metals and actinides, Geochim. Cosmochim. Acta 69 (2005) 875–892.
[3] M.H. Bradbury, B. Baeyens, Experimental measurements and modelling of sorption competition on montmorillonite, Geochim. Cosmochim. Acta 69 (2005) 4187–4197.
[4] P. Trivedi, L. Axe, J. Dyer, Adsorption of metal ions onto goethite: single-adsorbate and competitive systems, Colloids Surf. A 191 (1–2) (2001) 107–121.
[5] I. Heidmann, I. Christl, C. Leu, R. Kretzschmar, Competitive sorption of protons and metal cations onto kaolinite: experiments and modeling, J. Colloid Interface Sci. 282 (2005) 270–282.
[6] I. Christl, R. Kretzschmar, Competitive sorption of copper and lead at the oxide-water interface: implications for surface site density, Geochim. Cosmochim. Acta 63 (19/20) (1999) 2929–2938.
[7] D. Soltermann, M. Marques Fernandez, B. Baeyens, J.M. Brendlé, R. Dähn, Competitive Fe(II)–Zn(II) uptake on a synthetic montmorillonite, Environ. Sci. Technol. 48 (1) (2014) 190–198.
[8] J.P. Kaszuba, W.H. Runde, The aqueous geochemistry of neptunium: dynamic control of soluble concentrations with application to nuclear waste disposal, Environ. Sci. Technol. 33 (1999) 4427–4433.
[9] G. Choppin, Actinide speciation in the environment, J. Radioanal. Nucl. Chem. 273 (3) (2007) 695–703.
[10] Th. Rabung, Th. Stumpf, H. Geckeis, R. Klenze, J.I. Kim, Sorption of Am(III) and Eu(III) onto γ-alumina: experiment and modelling, Radiochim. Acta 88 (2000) 711–716.
[11] N. Huittinen, Th. Rabung, A. Schnurr, M. Hakanen, J. Lehto, H. Geckeis, New insight into Cm(III) interaction with kaolinite - influence of mineral dissolution, Geochim. Cosmochim. Acta 99 (2012) 100–109.
[12] T. Kupcik, Th. Rabung, J. Lützenkirchen, N. Finck, H. Geckeis, Th. Fanghänel, Macroscopic and spectroscopic investigations on Eu(III) and Cm(III) sorption onto bayerite (β-$Al(OH)_3$) and corundum (α-Al_2O_3), J. Colloid Interface Sci. 461 (2016) 215–222.
[13] G. Choppin, M. Jensen, Actinides in solution: Complexation and kinetics, 4th ed., in: L. Morss, N. Edelstein, J. Fuger (Eds.), The Chemistry of the Actinide and Transactinide Elements, vol. 4, Springer, Dordrecht, The Netherlands, 2010, pp. 2524–2621.
[14] N. Edelstein, J. Fuger, J. Katz, L. Morss, Summary and comparison of properties of the actinide and transactinide elements, 4th ed., in: L. Morss, N. Edelstein, J. Fuger (Eds.), The Chemistry of the Actinide and Transactinide Elements, vol. 3, Springer, Dordrecht, The Netherlands, 2010, pp. 1753–1835.
[15] D. Dzombak, F. Morel, Surface Complexation Modeling: Hydrous Ferric Oxide, Wiley, USA, 1990.
[16] X. Yang, Z. Sun, D. Wang, W. Forsling, Surface acid-base properties and hydration/dehydration mechanism of aluminum (hydr)oxides, J. Colloid Interface Sci. 308 (2007) 395–404.
[17] D.C. Koningsberger, R. Prins, X-Ray Absorption: Principles, Applications, Techniques of EXAFS, SEXAFS, and XANES, John Wiley & Sons, New York, NY, 1988.
[18] T. Ressler, WinXAS: a program for X-ray absorption spectroscopy data analysis under MS-Windows, J. Synchrotron Radiat. 5 (1998) 118–122.

[19] A.L. Ankudinov, B. Ravel, J. Rehr, S.D. Conradson, Real-space multiple-scattering calculation and interpretation of x-ray-absorption near-edge structure, Phys. Rev. B 58 (1998) 7565–7576.
[20] G. Bunker, Introduction to XAFS: A Practical Guide to X-Ray Absorption Fine Structure Spectroscopy, Cambridge University Press, NY, USA, 2010.
[21] M. Newville, Fundamentals of XAFS, Rev. Mineral. Geochem. 78 (1) (2014) 33–74.
[22] K. Gückel, A. Rossberg, K. Müller, V. Brendler, G. Bernhard, H. Foerstendorf, Spectroscopic identification of binary and ternary surface complexes of Np(V) on gibbsite, Environ. Sci. Technol. 47 (24) (2013) 14418–14425.
[23] J.A. Davis, D.B. Kent, Surface complexation modelling in aqueous geochemistry, Rev. Mineral. 23 (1990) 177–260 (M.F. Hochella, A.F. White (Eds.), Mineral-Water Interface Geochemistry.
[24] D.L. Parkhurst, C.A.J. Appelo, Description of input and examples for PHREEQC version 3–a computer program for speciation, batch- reaction, one-dimensional transport, and inverse geochemical calculations, U.S. Geological Survey Techniques and Methods, 2013 (Book 6, Chapter A43).
[25] E.P. Poeter, M.C. Hill, E.R. Banta, S. Mehl, S. Christensen, UCODE_2005 and six other computer codes for universal sensitivity analysis, calibration, and uncertainty evaluation, U.S. Geological Survey Techniques and Methods, 2005 (Book 6, Chapter A11).
[26] R.J. Lemire, J. Fuger, K. Spahiu, H. Nitsche, J.C. Sullivan, W.J. Ullman, P. Potter, P. Vitorge, M.H. Rand, H. Wanner, J. Rydberg, Chemical Thermodynamics of Neptunium and Plutonium, Elsevier, Amsterdam, 2001. 845.
[27] R. Guillaumont, T. Fanghänel, J. Fuger, I. Grenthe, V. Neck, D.A. Palmer, M.H. Rand, Update on the Chemical Thermodynamics of U, Np, Pu, Am. and Tc, Elsevier, Amsterdam, 2003. 970.
[28] M.M. Benjamin, J.O. Leckie, Multiple-site adsorption of Cd, Cu, Zn. and Pb on amorphous iron oxyhydroxide, J. Colloid Interface Sci. 79 (1) (1981) 209–221.
[29] B. Baeyens, M.H. Bradbury, A mechanistic description of Ni and Zn sorption on Na-montmorillonite Part I: titration and sorption measurements, J. Contam. Hydrol. 27 (1997) 199–222.
[30] M. Del Nero, B. Made, G. Bontems, A. Clement, Adsorption of neptunium(V) on hydrargilite, Radiochim. Acta 76 (1997) 219–228.
[31] M. Del Nero, K. Ben Said, B. Made, A. Clement, G. Bontems, Effect of pH and carbonate concentration in solution on the sorption of neptunium(V) by hydrargilite: application of the non-electrostatic model, Radiochim. Acta 81 (1998) 133–141.
[32] J.A. Davis, M. Ochs, M. Olin, T.E. Payne, C.J. Tweed, NEA Sorption Project Phase II, Interpretation and Prediction of Radionuclide Sorption onto Substrates Relevant for Radioactive Waste Disposal Using Thermodynamic Sorption Models, OECD Publishing, Paris, France, 2005.
[33] M. Snow, P. Zhao, Z. Dai, A.B. Kersting, M. Zavarin, Neptunium(V) sorption to goethite at attomolar to micromolar concentrations, J. Colloid Interface Sci. 390 (1) (2013) 176–182.
[34] P. Wang, A. Anderko, D.R. Turner, Thermodynamic modeling of the adsorption of radionuclides on selected minerals. I: Cations, Ind. Eng. Chem. Res. 40 (2001) 4428–4443.
[35] M. Newville, B. Boyanov, D. Sayers, Estimation of uncertainties in XAFS data, J. Synchrotron Radiat. 6 (1999) 264–265.
[36] O. Elo, K. Müller, A. Ikeda-Ohno, F. Bok, A.C. Scheinost, P. Hölttä, N. Huittinen, Batch sorption and spectroscopic speciation studies of neptunium uptake by montmorillonite and corundum, Geochim. Cosmochim. Acta. (2016) (submitted for publication).
[37] A. Ikeda-Ohno, C. Henning, A. Rossberg, H. Funke, A. Scheunost, G. Bernhard, T. Yaita, Electrochemical and complexation behaviour of neptunium in aqueous perchlorate and nitrate solutions, Inorg. Chem. 47 (2008) 8294–8305.
[38] K. Müller, A. Gröschel, A. Rossberg, F. Bok, C. Franzen, V. Brendler, H. Foerstendorf, In situ spectroscopic identification of neptunium(V) inner-sphere complexes on the hematite-water interface, Environ. Sci. Technol. 49 (2015) 2560–2567.
[39] Y. Arai, P.B. Moran, B.D. Honeyman, J.A. Davis, In situ spectroscopic evidence for neptunium(V)-carbonate inner-sphere and outer-sphere ternary surface complexes on hematite surface, Environ. Sci. Technol. 41 (2007) 3940–3944.
[40] T. Hattori, T. Saito, K. Ishida, A.C. Scheinost, T. Tsuneda, S. Nagasaki, S. Tanaka, The structure of monomeric and dimeric uranyl adsorption complexes on gibbsite: A combined DFT and EXAFS study, Geochim. Cosmochim. Acta 73 (20) (2009) 5975–5988.
[41] D. Sherman, C. Peacock, C. Hubbard, Surface complexation of U(VI) on goethite (a-FeOOH), Geochim. Cosmochim. Acta 72 (2008) 298–310.